Progress In Electromagnetics Research, PIER 11, 103–141, 1995

SOLUTION OF THE SCALAR HELMHOLTZ WAVE EQUATION BY LANCZOS REDUCTION

J. A. Fleck, Jr.

1. Introduction

The scalar Helmholtz equation is widely used in optics, acoustics, and geophysics to model propagation phenomena. Most applications rely on the paraxial or parabolic approximation to the Helmholtz equation for two reasons. First, the formal equivalence of the paraxial

wave equation and the Schrödinger equation creates a common ground for solution techniques that can be applied equally well to either wave propagation or quantum mechanics. Second, numerical solutions to the longitudinally first order paraxial wave equation can be generated numerically by marching algorithms, which are logically simple to implement and which minimize computer memory requirements. One marching technique, the split operator/fast Fourier-transform method [1], also known as the beam propagation method (BPM), has been widely applied to problems in atmospheric beam propagation and optoelectronics.

The paraxial approximation, unfortunately, breaks down under a variety of conditions, which apply to many interesting problems. Wide beam angles, steeply varying refractive index profiles, and propagation over long distances in multimode waveguides are examples of conditions that make the paraxial wave equation inaccurate. Our interest in this chapter is the development of accurate marching or one-way beam propagation algorithms for solving the Helmholtz equation that do not require invoking the usual paraxial approximations.

One-way beam propagation can only be postulated, strictly speaking, for longitudinally invariant refractive index profiles. In this chapter we make the assumption that longitudinal refractive index variations are sufficiently weak to make one-way beam propagation a good approximation. This assumption will enable us to concentrate on the wide-angle aspects of beam propagation. One can of course develop bidirectional solutions valid for all longitudinally varying index profiles by appealing to a solution of the corresponding time-dependent wave equation at the expense of adding another dimension (time) to the problem [2]. For problems involving propagation in three-dimensional waveguide structures spatial gridding requirements are frequently exacting enough to render time-domain treatments impractical. The search for wide-angle one-way beam propagation algorithms is thus well justified.

A number of modifications have been proposed to extend the accuracy of standard paraxial numerical methods to wider angles. One of these is due to Claerbout [3], who approximated the square root operator, which results in the factored form of the Helmholtz equation, by a four parameter rational function. The resulting pseudo-differential wave equation must be implemented in conjunction with an implicit finite-difference numerical scheme. This method has been

further refined by Lee, Saad, and Schultz [4]. A wide-angle variant of the standard paraxial split-operator BPM was proposed for propagation in optical waveguides by Feit and Fleck [5] and by Van Roey, Van der Donk, and Lagasse [6]. This same scheme was later employed by Feit and Fleck to study self-focusing in Kerr-active nonlinear media [7]. The wide-angle split-operator scheme follows the standard paraxial operator split of [1], with substitution of an exponentiated square root propagator for the paraxial propagator in the homogeneous medium propagation step of the algorithm. The accuracy of this scheme was studied by Thomson and Chapman [8] for underwater acoustic problems, who found the method to be accurate for beam angles up to about 24 degrees.

A one-way solution of the Helmholtz equation by matrix diagonalization was demonstrated by Thylén and Lee [9]. Since this method requires diagonalization of an $N' \times N'$ matrix, where N' is the number of grid points, it is practical only for waveguide configurations describable in one transverse dimension. The method of lines [10] is capable of generating Helmholtz solutions for certain three-dimensional waveguides, having special cross-sectional geometries, by diagonalization of matrices of comparable in size to those applicable in [9].

Our interest here is in modeling three-dimensional waveguides with arbitrary cross-sectional geometries, describable on $N' \times N'$ transverse grids, where N' is not necessarily a small number. For these waveguide systems the matrix diagonalization in the complete N'^2-dimensional space becomes impractical. If, however, one is interested in following the field over a limited propagation distance, it is possible to represent the N'^2-dimensional solution vector in terms of a small number of N'^2-dimensional orthogonal basis vectors, typically less than ten. These vectors in turn span a low-dimensional subspace, in which it is possible to determine the solution vector by diagonalizing a much lower order matrix than is required for unrestricted matrix diagonalization. Such subspaces, which we will refer to as Lanczos subspaces, were introduced by Lanczos [11], in the development of his method for determining extremal eigenvalues and their corresponding eigenvectors for very large matrices.

The Lanczos subspace concept has proven to be a powerful tool for solving both the time-dependent Schrödinger equation and the Helmholtz equation. To solve the time-dependent Schrödinger equation for a time-independent Hamiltonian operator one advances the

solution for the wave function $\Psi(t)$ over a time increment Δt by the operation $\Psi(\Delta t) = \exp(-iH\Delta g)\Psi(0)$, where H is the Hamiltonian operator. If one represents the wave function as an expansion in a set of basis functions u_n, the effect of the exponentiated operator can be conveniently computed by representing H as a matrix and diagonalizing it. For a large number of basis functions this diagonalization may be impractical. Park and Light [12] showed that the problem becomes tractable when one introduces a much smaller set, namely, the Krylov vectors, $\Psi(0), H\psi(0), \cdots, N^N\Psi(0)$, which form a Krylov space, and from the Krylov vectors constructs a set of orthogonal vectors by means of the Lanczos procedure [11,13]. These Lanczos vectors form a subspace in which the matrix representation of H is low order, and diagonalization is trivial. Iterative Lanczos reduction, as Park and Light called their scheme, was tested against other time-propagation methods for the Schrödinger equation and found to be capable of extremely low phase as well as amplitude errors [14].

It should also be expected that Lanczos reduction would serve as an accurate and efficient representation of the exponentiated square root operator in the relation

$$\Psi(\Delta t) = \exp\left\{ik\Delta z[1 - (1 + 2H/k)^{1/2}]\right\}\Psi(0),$$

which represents a formal one-way solution to the Helmholtz equation for a longitudinally invariant refractive index. This has indeed been shown to be the case by Ratowsky and Fleck [15] and Ratowsky, Fleck, and Feit [16,17], who have tested the method for a variety of longitudinally invariant waveguide structures. The original formulation of Lanczos reduction [12] was intended to apply only to Hermitian operators H, which are standard to quantum mechanics. In acoustics, however, attenuation may play an important role, and in optics both attenuation and gain can play important roles. At the very least, propagation is normally modeled by placing an absorbing boundary around the computational grid to inhibit boundary reflections. In modeling wave propagation, one therefore needs to generalize the standard Lanczos reduction to complex operators H. This generalization entails development of a bi-orthogonal Lanczos representation, which includes a set of right vectors and a set of left vectors whose components are not necessarily the complex conjugates of each other. It has been shown that a bi-orthogonal form of Lanczos reduction reproduces analytic results for both strong absorption and strong gain with high accuracy in

longitudinally invariant waveguides [17].

The Lanczos reduction method was employed in conjunction with the square root propagation operator by Hermansson et. al. [18] to analyze a semi-conductor rib-waveguide Y-junction device. These authors reported that a very small propagation step was necessary for numerical convergence, if the square root operator is used in conjunction with the Lanczos scheme. It would, however, be problematic to extrapolate the authors' results and conclusions for this device to all z-dependent devices, as they do. These authors also question the appropriateness of the Krylov space for diagonalization of the square root propagation operator in general. This conclusion certainly cannot be generally true because it is refuted by the accuracy of results obtained for specific longitudinally invariant waveguides, in which the Lanczos reduction method applied to the square root operator gives excellent agreement with analytic results.[15–17]. It will be shown in Sec 11 that convergence difficulties attributed to the perverse properties of the square root operator in [18] are due to the presence of evanescent components.

2. Solution of the Helmholtz Equation in Terms of a Square Root Operator

We shall be concerned with the scalar electric field $\Psi(x, y, z)$, which satisfies the scalar Helmholtz equation

$$\frac{\partial^2 \Psi}{\partial x^2} + \frac{\partial^2 \Psi}{\partial y^2} + \frac{\partial^2 \Psi}{\partial z^2} + \frac{n^2(x, y, z)}{c^2} \Psi = 0 \tag{1}$$

For the present we assume that the refractive index depends only on the transverse coordinates x and y. Later we can relax this assumption and assume that the refractive index can depend weakly on the longitudinal coordinate, z, i.e., so long as back reflection is weak. It will be convenient, although by no means necessary for the application of the Lanczos method, to factor a carrier wave from the field. Thus we write $\Psi(x, y, z) = \exp(-ikz)\Psi(x, y, z)$, where $k = \omega n_0/c$ and n_0 is a reference refractive index. Substitution of this expression for Ψ into Eq. (1) gives the following equation for Ψ.

$$-\frac{1}{2k}\frac{\partial^2 \Psi}{\partial z^2} + i\frac{\partial \Psi}{\partial z} = \frac{1}{2k}\nabla_\perp^2 \Psi + \frac{k}{2}\left(\frac{n^2(x, y)}{n_0^2} - 1\right)\Psi \tag{2}$$

Neglect of the second z-derivative gives the paraxial wave equation

$$i\frac{\partial \Psi}{\partial z} = \frac{1}{2k}\nabla_{\perp}^2 \Psi + \frac{k}{2}\left(\frac{n^2(x,y)}{n_0^2} - 1\right) \tag{3}$$

Equations (2) and (3) can be conveniently rewritten as follows

$$-\frac{1}{2k}\frac{\partial^2 \Psi}{\partial z^2} + i\frac{\partial \Psi}{\partial z} = H\Psi \tag{4a}$$

$$i\frac{\partial \Psi}{\partial z} = H\Psi \tag{4b}$$

where the operator H is defined by

$$H = \frac{1}{2k}\nabla_{\perp}^2 \Psi + \frac{k}{2}\left(\frac{n^2(x,y)}{n_0^2} - 1\right) \tag{5}$$

Equation (4a), which has the form of a kind of generalized Schrödinger equation, can be written in the factored form

$$\left[\frac{\partial}{\partial z} - ik - ik(1+2H/k)^{1/2}\right]\left[\frac{\partial}{\partial z} - ik + ik(1+2H/k)^{1/2}\right]\Psi$$
$$= ik\left[\frac{\partial}{\partial z}(1+2H/k)^{1/2} - (1+2H/k)^{1/2}\frac{\partial}{\partial z}\right]\Psi \tag{6}$$

Since, by assumption, H is independent of z, the righthand side of Eq. (6) vanishes, and Eq. (6) can be satisfied if either factor on the lefthand side is set equal to zero. The equation

$$\left[\frac{\partial}{\partial z} - ik + ik(1+2H/k)^{1/2}\right]\Psi = 0 \tag{7}$$

corresponds to a wave moving from left to right. Setting the remaining factor equal to zero gives the equation corresponding to a wave moving from right to left.

The solution to Eq. (7) can be expressed formally as

$$\Psi(z) = \exp\left\{ikz\left[1 - (1+2H/k)^{1/2}\right]\right\}\Psi(0) \tag{8}$$

Equation (8) is the basic equation that we will use in developing a one-way solution to the Helmholtz equation. In the limit that the expansion

$$(1+2H/k)^{1/2} \cong 1 + H/k \tag{9}$$

is a good approximation, Eq. (8) becomes

$$\Psi(z) = \exp(-iHz)\Psi(0)$$
$$= \exp\left\{-iz\left[\frac{1}{2k}\nabla_\perp^2 + \frac{k}{2}\left(\frac{n^2(x,y)}{n_0^2} - 1\right)\right]\right\}\Psi(0) \qquad (10)$$

Equation (10) represents a formal solution to the paraxial wave equation (3) that can be expressed to second order in commutation errors over a small propagation step Δz in the symmetrically split form

$$\Psi(0) = \exp(-\frac{i\Delta z}{4k}\nabla_\perp^2)\exp\left\{-\frac{ik\Delta z}{2}\left(\frac{n^2}{n_0^2} - 1\right)\right\}$$
$$\cdot \exp\left(-\frac{i\Delta z}{4k}\nabla_\perp^2\right) + O\left((\Delta z)^3\right) \qquad (11)$$

Equation (11) represents the well known BPM algorithm [1].

3. Numerical Solution by Matrix Diagonalization

We shall be interested in the finite basis of normalized plane wave functions

$$u_{mn}(x,y) = \frac{1}{L^2}\exp\left[\frac{2\pi i}{L}(mx + ny)\right],$$
$$-\frac{N'}{2} < m < \frac{N'}{2}, \qquad -\frac{N'}{2} < n < \frac{N'}{2} \qquad (12)$$

defined on an $N' \times N'$ square grid of side L. In this representation the field can be expressed by the finite Fourier series

$$\Psi(x,y,z) = \sum_{m=-N'/2+1}^{N'/2} \sum_{n=-N'/2+1}^{N'} B_{mn}(z)\exp\left[\frac{2\pi i}{L}(mx + ny)\right] \qquad (13)$$

where the set of all values $B_{mn}(z)$ can be regarded as an N'^2-dimensional vector $\boldsymbol{\Psi}(z)$ [9,17]. If we form an $N'^2 \times N'^2$ matrix $\mathbf{H}$ from the elements $< mn|H|m'n' >$, defined in the usual complex Hilbert space sense, Eqs. (4a) and (4b) reduce to

$$-\frac{1}{2k}\frac{\partial^2 \boldsymbol{\Psi}}{\partial z^2} + i\frac{\partial \boldsymbol{\Psi}}{\partial z} = \mathbf{H}\boldsymbol{\Psi} \tag{14a}$$

$$i\frac{\partial \boldsymbol{\Psi}}{\partial z} = \mathbf{H}\boldsymbol{\Psi} \tag{14b}$$

If we make the assumption that $\mathbf{H}$ is an Hermitian matrix, we can solve Eq. (14a) by applying Eq. (8), and we can solve Eq. (14b) by applying Eqs. (8) and (10) with the results

$$\boldsymbol{\Psi}(z) = \mathbf{U}^\dagger \mathbf{U} \exp\left\{ikz\left[1-(1+2\mathbf{H}/k)^{1/2}\right]\right\}\mathbf{U}^\dagger\mathbf{U}\boldsymbol{\Psi}(0) \tag{15a}$$

$$\boldsymbol{\Psi}(z) = \mathbf{U}^\dagger \mathbf{U} \exp\{-i\mathbf{H}z\}\mathbf{U}^\dagger\mathbf{U}\boldsymbol{\Psi}(0) \tag{15b}$$

where $\mathbf{U}$ and its Hermitian conjugate $\mathbf{U}^\dagger$ diagonalize the matrix $\mathbf{H}$, according to

$$\boldsymbol{\beta}' = diag[\beta'_1, \beta'_2, \cdots, \beta'_{N'^2}] = \mathbf{U}\mathbf{H}\mathbf{U}^\dagger \tag{16}$$

Here $\beta'_1, \beta'_2, \beta'_{N'^2}$ are the eigenvalues of $\mathbf{H}$ in this particular representation, and $\mathbf{U}$ and $\mathbf{U}^\dagger$ satisfy the relation $\mathbf{U}\mathbf{U}^\dagger = \mathbf{1}$, where $\mathbf{1}$ is the identity matrix. If we make use of Eq. (16), we can express Eqs. (15a) and (15b) in the following forms

$$\boldsymbol{\Psi}(z) = \mathbf{U}^\dagger \exp\left\{ikz\left[1-(1+2\boldsymbol{\beta}'/k)^{1/2}\right]\right\}\mathbf{U}\boldsymbol{\Psi}(0) \tag{17a}$$

$$\boldsymbol{\Psi}(z) = \mathbf{U}^\dagger \exp\left\{-i\boldsymbol{\beta}' z\right\}\mathbf{U}\boldsymbol{\Psi}(0) \tag{17b}$$

which are suitable for computation.

We recall that the solutions (17a) and (17b) are expressed in the momentum or plane-wave representation. The components of the vector $\boldsymbol{\Psi}(z)$ are the coefficients $B_{mn}(z)$, and therefore the components of $\boldsymbol{\Psi}$ can be converted to function values on the grid in direct space

by an inverse discrete Fourier transform. The eigenvectors of **H**, which are equivalent to the columns of the transformation matrix **U**, represent the bound and radiation modes that can be represented on the assumed computational grid. These eigenvectors can likewise be converted to function values on the spatial grid by an inverse discrete Fourier transform.

4. Application of the Krylov Space to Solution of the Helmholtz Equation

The above technique, while possible in principle, is impractical for any but the sparsest grids. If, for example, one is dealing with a 256×256 transverse grid, which represents a rather common size, it becomes necessary to diagonalize a $65,537 \times 65,537$ matrix. Out of necessity we are led to avoid dealing with the complete $N' \times N'$-dimensional Hilbert space and to express the solution vector in a much lower dimensional space. One possible space to employ for this purpose is the Krylov space formed, by the vectors $\mathbf{\Psi}(0)$, $\mathbf{H}\mathbf{\Psi}(0)$, $\cdots \mathbf{H}^N \mathbf{\Psi}(0)$, where $N << N'$.

This space is suggested for the Schrödinger or paraxial wave equation (14b) by the following argument [12]. The solution to Eq.(14b) can be approximated at $z = \Delta z$ by the Taylor expansion to order N

$$\begin{aligned}\mathbf{\Psi}(\Delta z) &= \exp(-i\Delta z \mathbf{H})\mathbf{\Psi}(0) \\ &= \sum_{n=0}^{N} \frac{1}{n!}(-ik\Delta z \mathbf{H})^n \mathbf{\Psi}(0) + O\left((\Delta z)^{N+1}\right)\end{aligned} \tag{18}$$

Since this finite series can be represented as a linear combination of the $N+1$ Krylov vectors, one can argue that to order N in Δz the Krylov vectors span the solution space of $\mathbf{\Psi}(\Delta z)$.

The corresponding argument unfortunately cannot be applied to the solution to the Helmholtz equation (8), which can be approximated to order N in Δz by the Taylor series expansion

$$\mathbf{\Psi}(\Delta z) = \sum_{n=0}^{N} \frac{1}{n!} \left\{ ik\Delta z \left[1 - (1 + 2\mathbf{H}/k)^{1/2}\right]\right\}^n \mathbf{\Psi}(0) + O\left((\Delta z)^{N+1}\right) \tag{19}$$

Even though expression (19) is accurate to order N in Δz, it contains implicitly all powers of $\mathbf{H}$ through the presence of the square root operator. Thus the Taylor series expansion of the solution vector cannot be represented as a linear combination of the $N+1$ Krylov vectors, and there is no guarantee that these vectors span the solution space to order N. If, on the other hand, the square root in expression (19) is expanded in a Taylor series in $\mathbf{H}$ to maximum order p, expression (19) can be represented as a linear combination of N_p Krylov vectors, and one can argue that the solution space is spanned to order N. These are admittedly plausibility arguments. Justification of the Krylov space, based on the matrix operator $\mathbf{H}$, for solving the Helmholtz equation must ultimately depend on the accuracy of numerical results obtained in specific practical applications.

5. Solution of the Helmholtz Equation for Hermitian H by Iterative Lanczos Reduction

The Krylov vectors themselves do not form an orthogonal set, but by applying the Lanczos orthogonalization procedure [11,13] one can derive an orthogonal set from them. It should be understood that the formation of an orthogonal set is not unique, but the Lanczos set is often favored because it leads to a symmetric tri-diagonal representation. For the moment we assume that $\mathbf{H}$ is Hermitian, and later we shall generalize the analysis to apply when $\mathbf{H}$ is nonHermitian.

To derive a set of $N+1$ orthonormal vectors $q_0, q_1, \cdots, q_n$ from the $N+1$ Krylov vectors $\mathbf{\Psi}(0)$, $\mathbf{H}\mathbf{\Psi}(0)$, $\cdots \mathbf{H}^N \mathbf{\Psi}$ (0) we begin by setting

$$q_0 = \mathbf{\Psi}(0) \tag{20}$$

In Figure 1 we show the projection of $\mathbf{H}\,q_0$ along q_0 and the as yet to be determined vector q_1. We can express the vector $\mathbf{H}\,q_0$ in terms of its projections along q_0 and q_1 as follows

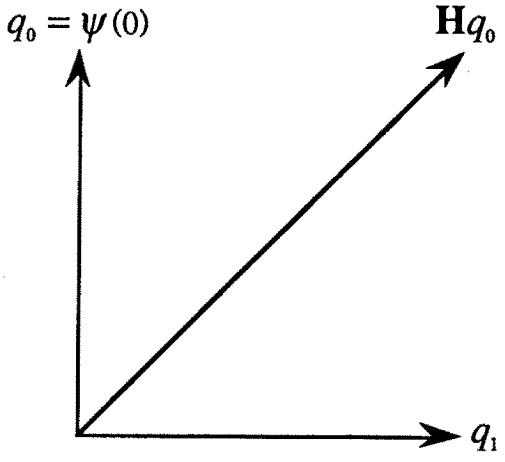

Figure 1. Projection of the vector H_{q_0} along orthogonal axes q_0 and q_1.

$$\mathbf{H}q_0 = \langle q_0|\mathbf{H}|q_0\rangle q_0 + \langle q_1|\mathbf{H}|q_0\rangle q_1 \tag{21}$$

For the basis (12) we can evaluate the projections in terms of discrete Fourier transforms as described in [1]. If we rename the projections

$$\alpha_0 = \langle q_0|\mathbf{H}|q_0\rangle, \quad \beta_0 = \langle q_1|\mathbf{H}|q_0\rangle \tag{22}$$

we can rewrite Eq. (21) as

$$\mathbf{H}q_0 = \alpha_0 q_0 + \beta_0 q_1 \tag{23}$$

or, equivalently,

$$\mathbf{H}q_0 - \alpha_0 q_0 = \beta_0 q_1 \tag{24}$$

If we impose the normalization condition $|q_1|^2 = 1$, we obtain

$$|\mathbf{H}q_0 - \alpha_0 q_0|^2 = |\beta_0|^2 \tag{25}$$

If we assume the phase of β_0 to be zero, q_1 is determined from Eq. (24) as

$$q_1 = (\mathbf{H}q_0 - \alpha_0 q_0)/\beta_0 \tag{26}$$

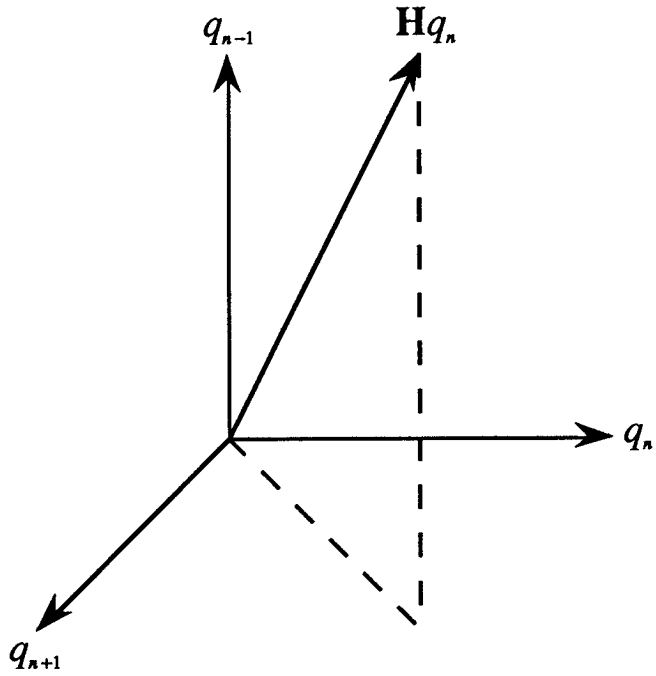

Figure 2. Projection of the vector H_{q_0} along orthogonal axes q_{n-1}, q_n and q_{n+1}.

For arbitrary n we can express $\mathbf{H}\,q_n$ in terms of its projections along q_{n+1}, q_n, and q_{n+1}, as is shown in Fig. 2. The corresponding equation is

$$\mathbf{H}q_n = \langle q_{n-1}|\mathbf{H}|q_n\rangle q_{n-1} + \langle q_n|\mathbf{H}|q_n\rangle q_n + \langle q_{n+1}|\mathbf{H}|q_n\rangle q_{n+1} \qquad (27)$$

For $n = 1$ Eq. (27) implies that q_0, q_1, and q_2 are orthogonal. By induction one can then show that all vectors in the set $q_0, q_2, \cdots, q_N$ are orthonormal. Since $\mathbf{H}$ is Hermitian, the matrix elements satisfy $\langle q_{n-1}|\mathbf{H}|q_n\rangle = \langle q_n|\mathbf{H}|q_{n-1}\rangle = \beta_{n-1}$. If we call $\langle q_n|\mathbf{H}|q_n\rangle = \alpha_n$, Eq. (27) can be written

$$\mathbf{H}q_n = \beta_{n-1}q_{n-1} + \alpha_n q_n + \beta_n q_{n+1} \qquad (28)$$

Making use of the normalization of q_{n+1}, we obtain from Eq. (28)

$$|\mathbf{H}q_n - \beta_{n-1}q_{n-1} - \alpha_n q_n|^2 = |\beta_n|^2 \tag{29}$$

The vector q_{n+1} can now be determined from Eq. (28) to be

$$q_{n+1} = (\mathbf{H}q_n - \beta_{n-1}q_{n-1} - \alpha_n q_n)/\beta_n \tag{30}$$

Once all of the vectors $q_0, q_2, \cdots, q_N$ have been determined, the matrix representation of $\mathbf{H}$ in the Lanczos subspace is complete, and the corresponding matrix can be written as $(N+1)\times(N+1)$ the symmetric tri-diagonal matrix

$$\mathbf{H}_N = \begin{pmatrix} \alpha_0 & \beta_0 & 0 & \cdots & 0 & 0 \\ \beta_0 & \alpha_1 & \beta_1 & \cdots & 0 & 0 \\ 0 & \beta_1 & \alpha_2 & \cdots & 0 & 0 \\ . & . & . & \cdots & . & . \\ 0 & 0 & 0 & \cdots & \alpha_{N-1} & \beta_{N-1} \\ 0 & 0 & 0 & \cdots & \beta_{N-1} & \alpha_N \end{pmatrix} \tag{31}$$

In the Lanczos subspace the solutions to Eqs (4a) and(4b) can be expressed in direct analogy to Eqs. (17a) and (17b) as

$$\mathbf{\Psi}(\triangle z) = \mathbf{U}_N^{\dagger} \exp\left\{ik\triangle z\left[1-(1+2\boldsymbol{\beta}'_N/k)^{1/2}\right]\right\}\mathbf{U}_N\,\mathbf{\Psi}(0) \tag{32a}$$

$$\mathbf{\Psi}(\triangle z) = \mathbf{U}_N^{\dagger} \exp(-i\,\boldsymbol{\beta}'_N \triangle z)\mathbf{U}_N\,\mathbf{\Psi}(0) \tag{32b}$$

where

$$\boldsymbol{\beta}'_N = diag\{\beta'_1, \beta'_2, \cdots \beta'_N\} = \mathbf{U}_N\mathbf{H}_N\mathbf{U}_N^{\dagger}.$$

If the input field $\mathbf{\Psi}(0)$ is a linear superposition of exactly $N+1$ eigenvectors of $\mathbf{H}$, the $N+1$ dimensional Lanczos subspace, constructed from $\mathbf{\Psi}(0)$, becomes identical with the space spanned by these eigenvectors because we can construct only $N+1$ independent Krylov vectors and from these Krylov vectors only $N+1$ independent orthonormal Lanczos vectors. Clearly the diagonalization of the Matrix $\mathbf{H}_N$ will result in the original eigenvectors and eigenvalues.

Note that if the Lanczos recursion is terminated by setting $q_{n+1} = 0$ on the right hand side of Eq. (28), the left hand side of Eq. (29) is also zero. Thus the computed value of β_{n+1} will also be zero. The practical consequence of this fact is that if the value of β_{n+1}, computed from Eq. (29), turns out to be very small, that is very small in comparison with β_n, it may be useful to reduce the Lanczos order of the calculation by setting $q_{n+1} = 0$.

It is of interest to pursue the limit in which a field is propagating in a monomode waveguide, and most of the power in radiation modes has radiated away. The truncation described above requires setting $q_1 = 0, q_0 = \Psi(0)$, and

$$\mathbf{H}q_0 = \langle q_0|\mathbf{H}|q_0\rangle = \alpha_0 q_0 \tag{33}$$

The solutions (32a) and(32b) become

$$\Psi(\Delta z) = \exp\left\{ik\Delta z\left[1-(1+2\alpha_0/k)^{1/2}\right]\right\}\Psi(0) \tag{34a}$$

$$\Psi(\Delta z) = \exp(-i\alpha_0\Delta z)\,\Psi(0) \tag{34b}$$

which is the result obtainable from first order quantum mechanical perturbation theory.

6. Selection of a Propagation Step

The selection of the propagation step Δz may be based on an error estimate, determined by the magnitude of the projection on $\Psi(\Delta z)$ of the first vector coefficient q_{N+1}, lying outside the Lanczos subspace [12]. If, on the other hand, one wishes to pursue accurately a calculation to a given Lanczos order, employing the Lanczos vector set $q_0, q_2, \cdots, q_N$, it will be necessary to follow each of the phase factors,

$$\exp\left\{ik\Delta z\left[1-(1+2\beta_n'/k)^{1/2}\right]\right\}, \quad n = 1, 2, \cdots N \tag{35}$$

accurately through their respective periods of oscillation. Applying the phase-following criterion to the solutions (32a) and (32b), one obtains

the following criteria for the propagation steps corresponding to the Helmholtz and paraxial equations

$$\Delta z < \frac{\pi}{4}\mathrm{Min}\left|\frac{1}{\mathrm{Re}\left\{k\left[1-(1+2\beta_n'/k)^{1/2}/k\right]\right\}}\right| \tag{36a}$$

$$\Delta z < \frac{\pi}{4}\mathrm{Min}\left|\frac{1}{\beta_n'}\right| \tag{36b}$$

7. Decaying Solution Components

When

$$2\beta_n'/k < -1 \tag{37}$$

$(1+2\beta_n'/k)^{1/2}$ becomes pure imaginary, and the corresponding exponential, (35), decays exponentially. To study the implications of relation (37) we approximate a radiation mode by a plane wave and take $n \approx n_0$. We have from Eq. (5)

$$2\beta_n'/k \approx -(\kappa_x^2+\kappa_y^2)/k^2 \tag{38}$$

where κ_x and κ_y are the applicable transverse spatial frequencies. The angle between the direction of propagation of the plane wave and the z-axis is

$$\theta = \sin^{-1}(\kappa_x^2+\kappa_y^2)^{1/2}/k \tag{39}$$

Condition (37) implies that the plane wave cannot propagate in the forward direction, and the exponential (35) should be expected to decay exponentially.

For propagation in homogeneous media the above plane wave analysis becomes exact. Each Fourier component in the field is multiplied by a factor of the form (35). If a particular Fourier component of the field at $z = 0$ falls outside the propagation pass band, defined by Eqs. (37) and (39), its amplitude decays exponentially with propagation distance. For many initial fields one can expect a fraction of spectral power to lie outside the propagation pass band. For such initial fields the propagation problem is ill posed. The square root operator, on the other hand, acts as a filter that accepts only the "well

posed" components. If the square root operator is approximated by a finite Taylor series, however, the approximated square root can never be imaginary. Although the resulting propagation model becomes, in a sense, a wide-angle model, it cannot eliminate from the solution components that cannot properly propagate.

During transient phases of propagation in rib waveguides [16] the sharp transitions in the refractive index generate high spatial frequencies in the field. The highest frequencies generated are the highest frequencies that can be supported on the grid, that is, $\kappa_{max} = \sqrt{2\pi}/\Delta x$. Not all these components will be allowed to propagate by the square root operator, and power will be dissipated by the removal from the field of these nonpropagating components. The power dissipation can be expected to depend not only on grid parameters but on the Lanczos order as well, since the Lanczos modes are not the true modes of the system and may damp somewhat differently from the actual component plane waves. In a straight waveguide this filtering is of little concern because the unwanted spatial frequencies are dissipated in a short propagation distance. Every step of propagation in a z-dependent rib structure [18], on the other hand, represents a transient problem with fresh nonpropagating components being generated. Convergence of the calculated power loss with respect to Lanczos order and propagation step size may, as a consequence, not always appear monotonic. Convergence is improved if a truncated Taylor series is substituted for the square root operator [18], but accuracy is impaired because nonpropagating Fourier components are allowed to propagate with the field. We shall return to this general subject in Sec 11, where evanescent waves will be discussed.

8. Solution for a Bound Mode by Lanczos Iteration

A well known procedure for determining the bound mode of a monomode waveguide involves propagation of some input field using the paraxial wave equation (4b) with z replaced by iz. After propagation over a sufficiently long path the amplitudes of all unbound modes should decay exponentially relative to the bound mode amplitude. The paraxial eigenvalue can be computed from the expectation value $\langle \Psi(z)|H|\Psi(z)\rangle$, where $\Psi(z)$ is the final field. The Helmholtz eigenvalue can then be computed from the paraxial eigenvalue by a

square root transformation. One defect of this procedure is that an excessively long propagation path may be required to reduce significantly the amplitudes of the unwanted modes. A second defect is that the method provides no estimate of the error of the computed bound mode eigenvalue.

One can, on the other hand, construct an iterative scheme [16], based on the application of a sequence of Lanczos propagation steps that removes both of the shortcomings of the scheme based on propagation in imaginary z. The iteration proceeds as follows. Let $\Psi(0)$ be the input field vector and set $q_0 = \Psi(0)$. One constructs the orthonormal Lanczos vectors $q_0, q_1, \cdots, q_N$ and the matrix $\mathbf{H}_N$ using the procedure described in Sec. 5. Diagonalization of $\mathbf{H}_N$ generates eigenvalues $\beta'_0, \beta'_1, \cdots, \beta'_N$, where the eigenvalues are ordered so that $\beta'_0 > \beta'_1 > \cdots > \beta'_N$. For a monomode waveguide β'_0 will correspond to the bound mode and will be positive, while the remaining eigenvalues will be negative. Diagonalization also generates the transformation matrix $\mathbf{U}$, which can be expressed in terms of the eigenvectors of $\mathbf{H}_N$ by

$$\mathbf{U} = [\mathbf{u}_0 \mathbf{u}_1 \cdots \mathbf{u}_N] \tag{40}$$

Assuming that β'_0 and $\mathbf{u}_0$ are good approximations to the eigenvalue and eigenvector for the bound mode, one can discard the other eigenvectors and let $\mathbf{u}_0$ serve as the input field $q_0 = \Psi(0)$ for the next iteration. It is necessary, however, to express $\mathbf{u}_0$ in terms of the q-vectors. Thus the iteration scheme can be expressed in the form

$$q_0^{m+1} = \sum_{n=0}^{N} [\mathbf{u}_0]_n q_n^m \tag{41}$$

where m is an iteration number, and $[\mathbf{u}_0]_n$ represents a component of $\mathbf{u}_0$ in the dimensional subspace in which $\mathbf{H}_N$ is defined. The process leads to a successively weaker presence of all modes other than the desired bound mode. The procedure can be repeated until the solution has converged to the desired degree of accuracy, defined by the condition

$$\left| \frac{\beta'^{m+1}_0 - \beta'^{m}_0}{\beta'^{m}_0} \right| < \varepsilon \tag{42}$$

With the help of this iteration procedure it should be possible to achieve accuracy in a few tens to a few hundreds of iterations, involving less cost than would be incurred for a moderate length propagation calculation [16].

For a directional coupler formed from two monomode waveguides there are two bound modes, a symmetric mode and an anti-symmetric mode. Either mode can be computed by the above procedure by taking as the input field either a symmetric or an anti-symmetric function [16]. If the eigenvalues corresponding to the even and odd modes are, respectively, β'_{even} and β'_{odd}, the coupling length for the coupler can be determined using the relation

$$L_c = \pi/|\beta'_{\text{odd}} - \beta'_{\text{even}}| \tag{43}$$

9. Generalization of Lanczos Orthogonalization to NonHermitian Operators

We shall now consider the generalization of the operator (5) to nonHermitian form in which the refractive index profile is complex. Let us assume the form [17]

$$n(x, y) = n'(x, y)[1 + i\delta(x, y)] \tag{44}$$

Since the operator H is no longer Hermitian, it is necessary to employ the Lanczos orthogonalization procedure in biorthogonal form. To this end we define a set of "right" column vectors $|q_0\rangle, |q_1\rangle, \cdots, |q_N\rangle$ and a set of left row vectors $\langle q'_0|, \langle q'_1|, \cdots, \langle q'_N|$, where, in keeping with standard Dirac notation, the prime indicates that the components of the vector $\langle q'_n|$ are not the complex conjugates of the vector $|q_n\rangle$, unless the operator H is Hermitian. We wish the vectors, nonetheless, to remain mutually orthogonal according to the rule

$$\langle q'_n|q_{n'}\rangle = \delta_{nn'} \tag{45}$$

Figure 3 depicts the vectors $\mathrm{H}|q_N\rangle$ and $\langle q'_N|\mathrm{H}$ projected along three orthogonal axes in Hilbert spaces appropriate to right and left vectors, respectively. The corresponding equations describing these projections are

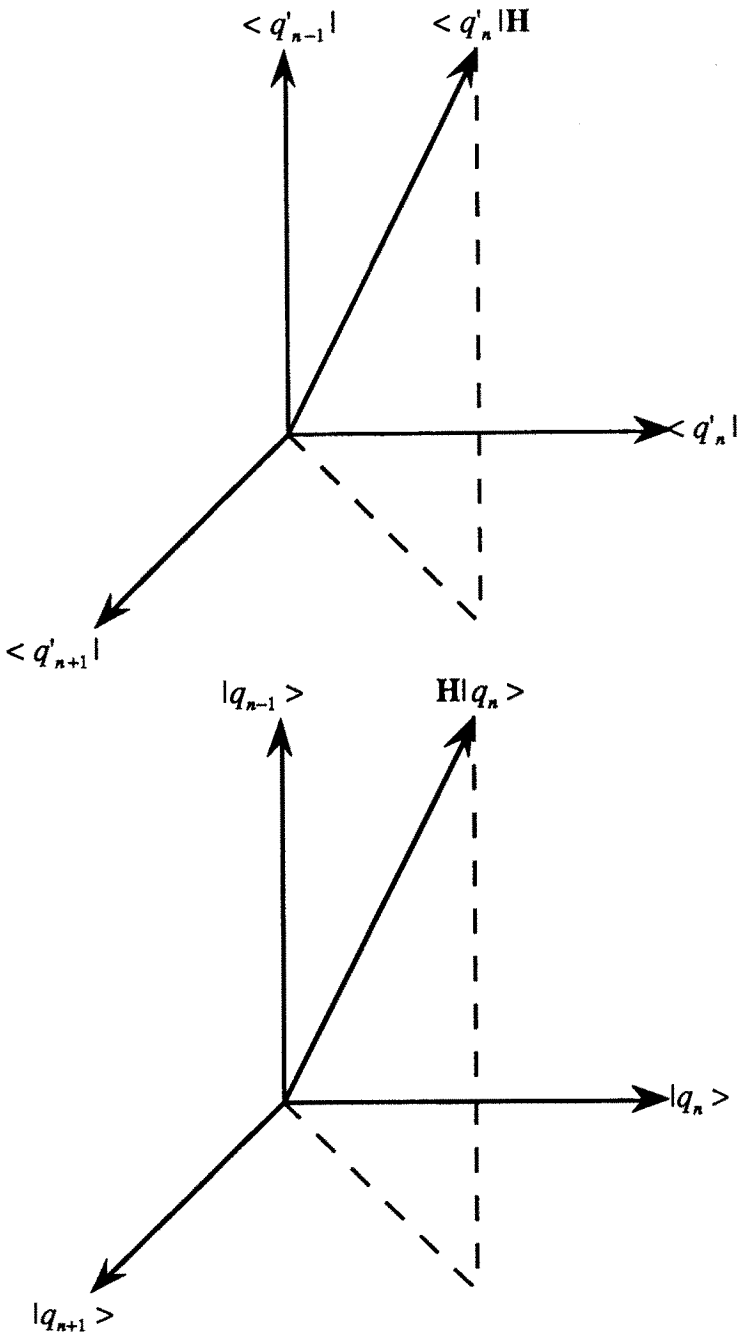

Figure 3. Projections of the right vector $\mathrm{H}|q_n\rangle$ and of the left vector $\langle q_n|\mathrm{H}$ along orthogonal axes in right and left space, respectively.

$$\mathbf{H}|q_n\rangle = \langle q'_{n-1}|\mathbf{H}|q_n\rangle|q_{n-1}\rangle + \langle q'_n|\mathbf{H}|q_n\rangle|q_n\rangle + \langle q'_{n+1}|\mathbf{H}|q_n\rangle|q_{n+1}\rangle \quad (46a)$$

$$\langle q'_n|\mathbf{H} = \langle q'_n|\mathbf{H}|q_{n-1}\rangle\langle q'_{n-1}| + \langle q'_n|\mathbf{H}|q_n\rangle\langle q_n| + \langle q'_n|\mathbf{H}|q_{n+1}\rangle\langle q'_{n+1}| \quad (46b)$$

Since the choice of the orthogonal vector sets is nonunique, we are free to pick the matrix elements so that the representation of $\mathbf{H}$ is symmetric. Thus we set

$$\begin{aligned} &|q_0\rangle = \Psi(0), \quad \langle q'_0| = \Psi^*(0) \\ &\langle q'_{n-1}|\mathbf{H}|q_n\rangle = \langle q'_n|\mathbf{H}|q_{n-1}\rangle = \beta_{n-1} \\ &\langle q'_{n+1}|\mathbf{H}|q_n\rangle = \langle q'_n|\mathbf{H}|q_{n+1}\rangle = \beta_n \\ &\langle q'_n|\mathbf{H}|q_n\rangle = \alpha_n \end{aligned} \quad (47)$$

and express Eqs. (46a) and (46b) in the form

$$\mathbf{H}|q_n\rangle = \beta_{n-1}|q_{n-1}\rangle + \alpha_n|q_n\rangle + \beta_n|q_{n+1}\rangle \quad (48a)$$

$$\langle q'_n|\mathbf{H} = \beta_{n-1}\langle q'_{n-1}| + \alpha_n\langle q'_n| + \beta_n\langle q'_{n+1}| \quad (48b)$$

We note that the right hand sides of Eqs. (48a) and (48b) are formally equivalent. The difference between the two equations lies in the form and method of evaluation of the left had sides. The left hand side of Eq. (48b) can be evaluated by using the identity

$$\langle q'_n|\mathbf{H} \equiv \left\{\mathbf{H}^\dagger|q'_n\rangle\right\}^\dagger \quad (49)$$

In Eq. (49) $\mathbf{H}^\dagger$ represents the adjoint or the transpose conjugate of $\mathbf{H}$, and, according to Dirac notation, the components of $|q'_n\rangle$ are the complex conjugates of the components of $\langle q'_n|$. It is also instructive to rewrite Eq. (48b) by taking the adjoint of both sides of the equation. The result is

$$\mathbf{H}^\dagger|q'_n\rangle = \beta_{n-1}|q'_{n-1}\rangle + \alpha_n|q'_n\rangle + \beta_n|q'_{n+1}\rangle \quad (50)$$

In the case that $\mathbf{H} = \mathbf{H}^\dagger$, the operator $\mathbf{H}$ is self-adjoint, Eqs. (48b) and (50) are equivalent, and $|q_n\rangle = |q'_n\rangle$.

One begins the determination of the vectors by setting

$$
\begin{aligned}
&|q_0\rangle = \Psi(0), \quad \langle q_0'| = \Psi^*(0) \\
&\mathbf{H}|q_0\rangle - \alpha_0|q_0\rangle = \beta_0|q_1\rangle \\
&\langle q_0'|\mathbf{H} - \alpha_0\langle q_0'| = \beta_0\langle q_1'|
\end{aligned} \tag{51}
$$

One now writes Eqs. (48a) and (48b) as

$$\mathbf{H}|q_n\rangle - \beta_{n-1}|q_{n-1}\rangle - \alpha_n|q_n\rangle = \beta_n|q_{n+1}\rangle \tag{52a}$$

$$\langle q_n'|\mathbf{H} - \beta_{n-1}\langle q_{n-1}'| - \alpha_n\langle q_n'| = \beta_n\langle q_{n+1}'| \tag{52b}$$

Taking the scalar product between the second and third of Eqs. (51), we obtain

$$\{\langle q_0'|\mathbf{H} - \alpha_0\langle q_0'|\}\{\mathbf{H}|q_0\rangle - \alpha_0|q_0\rangle\} = \beta_0^2 \tag{53}$$

Equation (53) determines β_0 to within a phase factor, which we set equal to unity. From the second and third of Eqs. (51) we obtain

$$
\begin{aligned}
|q_1\rangle &= (\mathbf{H}|q_0\rangle - \alpha_0|q_0\rangle)/\beta_0 \\
\langle q_1| &= (\langle q_0'|\mathbf{H} - \alpha_0\langle q_0'|)/\beta_0
\end{aligned} \tag{54}
$$

Similarly, we obtain from Eqs. (52a) and (52b)

$$
\begin{aligned}
\beta_n^2 &= \{\langle q_n'|\mathbf{H} - \beta_{n-1}\langle q_{n-1}'| - \alpha_n\langle q_n'|\}\{\mathbf{H}|q_n\rangle - \beta_{n-1}|q_{n-1}\rangle - \alpha_n|q_n\rangle\} \\
|q_n\rangle &= (\mathbf{H}|q_n\rangle - \beta_{n-1}|q_{n-1}\rangle - \alpha_n|q_n\rangle)/\beta_n \\
\langle q_n| &= (\langle q_n'|\mathbf{H} - \beta_{n-1}\langle q_{n-1}'| - \alpha_n\langle q_n'|)/\beta_n
\end{aligned} \tag{55}
$$

The matrix elements $\langle q_n'|\mathbf{H}|q_n\rangle$ form an $N+1$-dimensional symmetric tridiagonal representation for $\mathbf{H}$. The corresponding matrix, which we call $\mathbf{H}_N$, is identical in form to the matrix (31), but the diagonal elements will in general be complex for refractive indices that have the functional form of Eq. (44). We can now express the solution to either

the Helmholtz or the paraxial wave equations, in analogy with Eqs. (32a) and (32b), as

$$\Psi(\triangle z) = \mathbf{U}_N^{-1} \exp\left\{-ik\triangle z\left[1-(1+2\boldsymbol{\beta}'_N/k)^{1/2}\right]\right\}\mathbf{U}_N\Psi(0) \quad (56a)$$

$$\Psi(\triangle z) = \mathbf{U}_N^{-1}\exp(i\boldsymbol{\beta}'_N\triangle z)\mathbf{U}_N\Psi(0) \quad (56b)$$

where $\boldsymbol{\beta}'_N = diag\{\beta'_1, \beta'_2, \cdots, \beta'_N\} = \mathbf{U}_N\mathbf{H}_N\mathbf{U}_N^{-1}$.

Note that in writing Eqs. (56a) and (56b) we have changed the sign convention in the exponentials from that originally assumed for a right moving wave. We have done this to make it easier to select the decaying modes for those eigenvalues that correspond to decaying solutions in the absence of absorption.

10. Numerical Tests of Iterated Lanczos Reduction

Accuracy of bound modes in a quadratic waveguide

Iterated Lanczos reduction is designed to generate accurate solutions of propagation problems by substituting a low dimensional subspace for the high dimensional space that corresponds to the numerical grid used in the problem. One of the first questions one would like to have answered is the following. Can a computation that utilizes a few Lanczos vectors and, consequently, generates only a few Lanczos modes adequately describe the propagation of a field that is composed of many modes? To that end we consider following problem.

We consider the following one-dimensional multi-mode parabolic index profile

$$n^2 = n_1^2\left[1-2\triangle\left(\frac{x}{x_0}\right)^2\right], \quad x < x_0$$

$$n^2 = n_1^2(1-2\triangle), \qquad x \geq x_0 \quad (57)$$

with $n_0 = 1.5, \lambda = 0.9\mu m, k = 1.047 \times 10^5 cm^{-1}, \Delta = 0.031248$, and $x_0 = 60\mu m$. The input beam launched into the waveguide is

$$\Psi(0) = \sum_{n=0}^{25} N_n \exp(-x^2/2\sigma^2) H_n(x/\sigma)$$

$$\sigma = \left[\frac{x_0(1-2\Delta)}{2k\Delta}\right]^2 \tag{58}$$

where H_n and N_n are Hermite polynomials and normalization coefficients, respectively. Equation (58) represents the first 26 normalized eigenfunctions corresponding to the index profile [Eq. (57)] without cutoff. (The cutoff was included for numerical reasons).

The Lanczos reduction technique as described in Sec. 5 for Hermitian H was employed using five Lanczos vectors with $\Delta z = 3\mu m$ on a grid with 128 grid points, separated by $\Delta x = 0.14\mu m$. To study the mode structure of the beam the field correlation function has been computed using the expression

$$\mathcal{P}(z) = \int dx \Psi^*(x,0)\Psi(x,z) \tag{59}$$

To compute a mode spectrum [19] one computes the Fourier transform of the correlation function using

$$\mathcal{P}(\beta) = \frac{1}{Z}\int_0^z \exp(i\beta z)\mathcal{P}(z)w(z)dz \tag{60}$$

where

$$w(z) = 1 - \cos\left(\frac{2\pi}{Z}\right) \tag{61}$$

is a Hanning window function. If the field at longitudinal position z is expressed in terms of modes as

$$\Psi(x,z) = \sum_n A_n u_n(x) \exp(-i\beta_n z) \tag{62}$$

the spectrum computed using expression (60) takes the form

$$\mathcal{P}(\beta) = \sum_n |A_n|^2 \mathcal{L}(\beta - \beta_n') \tag{63}$$

where the line shape function $\mathcal{L}(\beta - \beta_n')$ is

$$\mathcal{L}(\beta - \beta_n')$$
$$= \frac{1}{Z}\int_0^z \exp[i(\beta - \beta_n')z]w(z)dz$$
$$= \frac{\exp[i(\beta - \beta_n')Z] - 1}{i(\beta - \beta_n')Z}$$
$$- \frac{1}{2}\left(\frac{\exp\{i[(\beta - \beta_n')Z] + 2\pi]\} - 1}{i[(\beta - \beta_n')Z + 2\pi]} + \frac{\exp\{i[(\beta - \beta_n')Z - 2\pi]\} - 1}{i[(\beta - \beta_n')Z - 2\pi]}\right) \tag{64}$$

The Helmholtz spectrum for this problem, shown in Fig. 4, clearly reveals 26 peaks, corresponding to the presence of all 26 modes. The position of the peaks, which does not in general lie on grid points in transform space, can be located accurately by an interpolation technique [19].

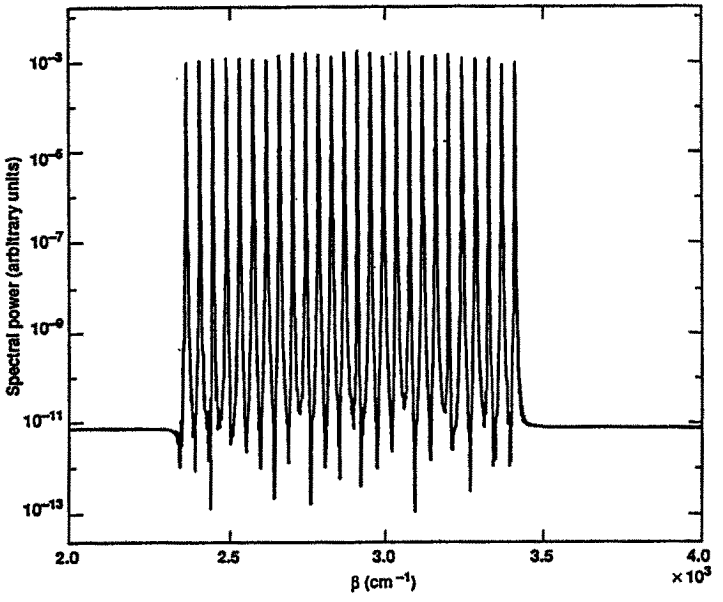

Figure 4. Mode spectrum for field containing 26 modes of equal amplitude, launched into a quadratic waveguide. Field is calculated using only 6 Krylov vectors in conjunction with the Lanczos method.

Paraxial	Analytic paraxial	Analytic Helmholtz	Numerical Helmholtz
3468.90431	0.90437	3431.27745	0.27755
3425.87269	0.87269	3371.59611	0.59618
3382.84102	0.84101	3329.89865	0.89861
3339.80931	0.80933	3288.18504	0.18516
3296.77766	0.77765	3246.45539	0.45537
3253.74597	0.74597	3204.70955	0.70954
3210.71425	0.71429	3162.94754	0.94768
3167.68261	0.68261	3121.16942	0.16942
3124.65092	0.65093	3079.37507	0.37507
3081.61921	0.61926	3037.56449	0.56462
3038.58757	0.58758	2995.73775	0.73782
2995.55588	0.55590	2953.89472	0.89468
2952.52418	0.52422	2912.03540	0.03544
2909.49254	0.49254	2870.15986	0.15994
2866.46085	0.46086	2828.26796	0.26803
2823.42915	0.42918	2786.35974	0.35971
2780.39751	0.39750	2744.43522	0.43518
2737.36581	0.36582	2702.49428	0.49433
2694.34112	0.34114	2660.53697	0.53709
2651.30247	0.30246	2618.56330	0.56338
2608.27076	0.27078	2576.57316	0.57316
2565.23907	0.23910	2534.56659	0.56657
2522.20742	0.20742	2492.54361	0.54357
2479.17571	0.17574	2450.50409	0.50411
2436.14403	0.14406	2408.44810	0.44816
2393.11239	0.11238	2366.37563	0.37568

Table 1. Propagation constants (in inverse centimeters) for 26 levels, obtained from six-vector Lanczos propagation for 8192 z-steps of $3.0\mu m$. The transverse grid used 128 points with $0.14\mu m$ spacing.

Table 1 illustrates the accuracy of the Lanczos propagation as determined by the numerical spectra such as that shown in Fig. 4. Displayed are: in the first column the mode eigenvalues, determined by the Lanczos method, used in conjunction with the paraxial wave equation (14b) and the line-shape equation (64); in the second column the analytic paraxial eigenvalues determined from the formula

$$\beta_n = \frac{\Delta n_1^2}{n_0}\frac{\omega}{c} - \frac{n_1}{n_0}\frac{(2\Delta)^{1/2}}{x_0}\left(n+\frac{1}{2}\right) \tag{65}$$

in the third column the Helmholtz eigenvalues, computed from the analytic paraxial eigenvalues using the formula [21]

$$\beta_H = k\left[1-(1+2\beta_{\text{parax}}/k)^{1/2}\right] \tag{66}$$

where β_H and β_{parax} are the Helmholtz and paraxial eigenvalues, respectively; and in the fourth column the five significant figures after the decimal for the numerically generated Helmholtz eigenvalues. Table 1 shows that the analytic and numerical paraxial eigenvalues and the analytic and numerical Helmholtz eigenvalues agree to seven or eight significant figures,respectively. This agreement together with the appearance of all 26 propagating modes in the numerical solution establish the Lanczos reduction method as an accurate tool for solving the Helmholtz equation in longitudinally invariant refractive media without absorption or gain.

Accuracy of Lanczos propagation in media with spatially dependent gain or loss

To test the accuracy of the nonHermitian Lanczos scheme, described in Sec. 9, we consider propagation in the complex parabolic refractive index profile [17]

$$\begin{aligned} n^2 &= n_1^2(1-i\nu)\left[1-2\Delta\left(\frac{x}{x_0}\right)^2\right], \quad x < x_0 \\ n^2 &= n_1^2(1-2\Delta), \qquad\qquad x \geq x_0 \end{aligned} \tag{67}$$

where all parameters are taken to be the same as for Eq. (54), and where ν positive describes a positive gain profile. An analytic solution

to the Helmholtz equation for the profile (67) without a cutoff can be expressed as

$$\Psi(x,z) = \sum_{n=0}^{N} A_n \Psi_n(x) \exp\left\{-ikz\left[1-(1+2\beta_n'/k)^{1/2}\right]\right\} \tag{68}$$

where

$$\Psi_n(x) = N_n \exp(-x^2/2\sigma^2) H_n(x/\sigma) \tag{69}$$

and

$$\sigma = \left[\frac{x_0(1-2\triangle)}{2k\triangle(1-i\nu)^2}\right]^{1/2} \tag{70}$$

In Eq. (66) β_n' are the paraxial eigenvalues

$$\beta_n' = \frac{\triangle n_1^2(1-i\nu)^2}{n_0}\frac{\omega}{c} - \frac{n_1(1-i\nu)}{n_0}\frac{(2\triangle)^{1/2}}{x_0}\left(n+\frac{1}{2}\right) \tag{71}$$

and in Eq. (69) N_n and H_n are normalization constants and Hermite polynomials. The eigenfunctions (69) are accurate as long as the modes are not too close to cutoff.

The initial condition is assumed to be

$$\Psi(x,0) = \sum_{n=0}^{25} \Psi_n(x_1)\Psi_n(x) \tag{72}$$

which represents a finite width δ-function, offset from the z-axis to $x = x_1$. We have taken $x_1 = 20\mu m$ and the grid parameters and Δz the same as for the previous example. The parameter ν was selected so that the gain or loss length have the value $0.05cm$ at the center of the waveguide.

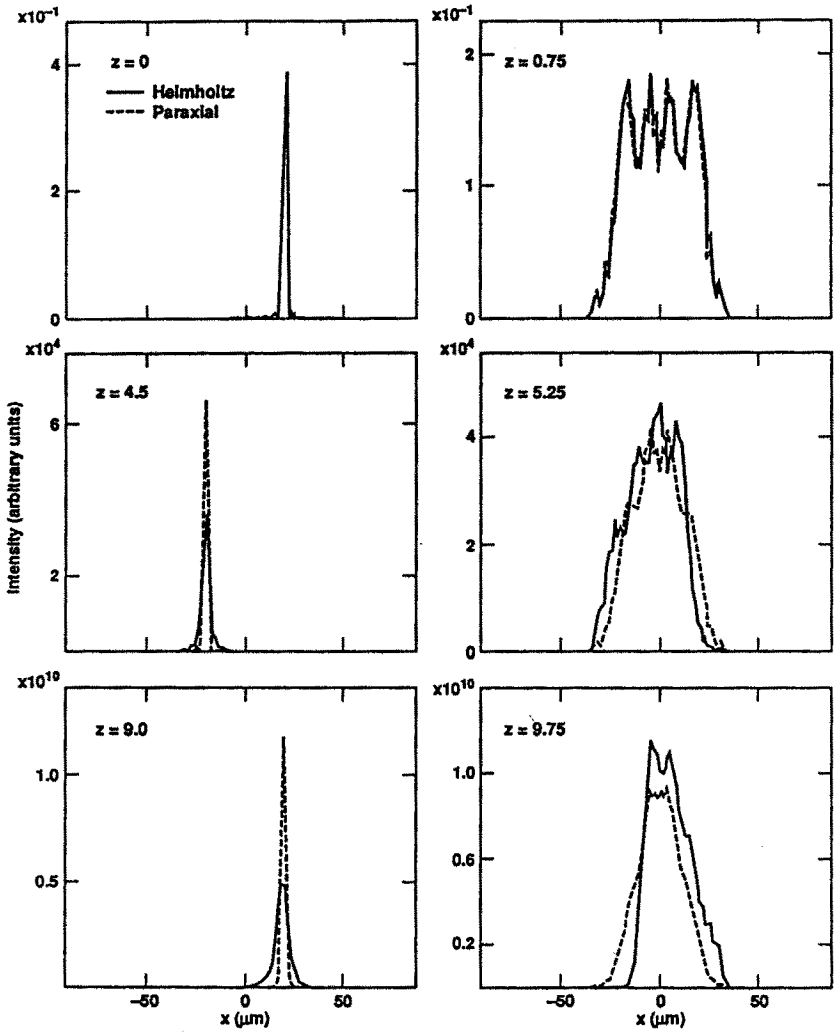

Figure 5. Comparison between Helmholtz and paraxial propagation in a quadratic refractive index waveguide with a quadratic gain profile. Analytic and numerical solutions of Helmholtz equation are superimposed and indistinguishable.

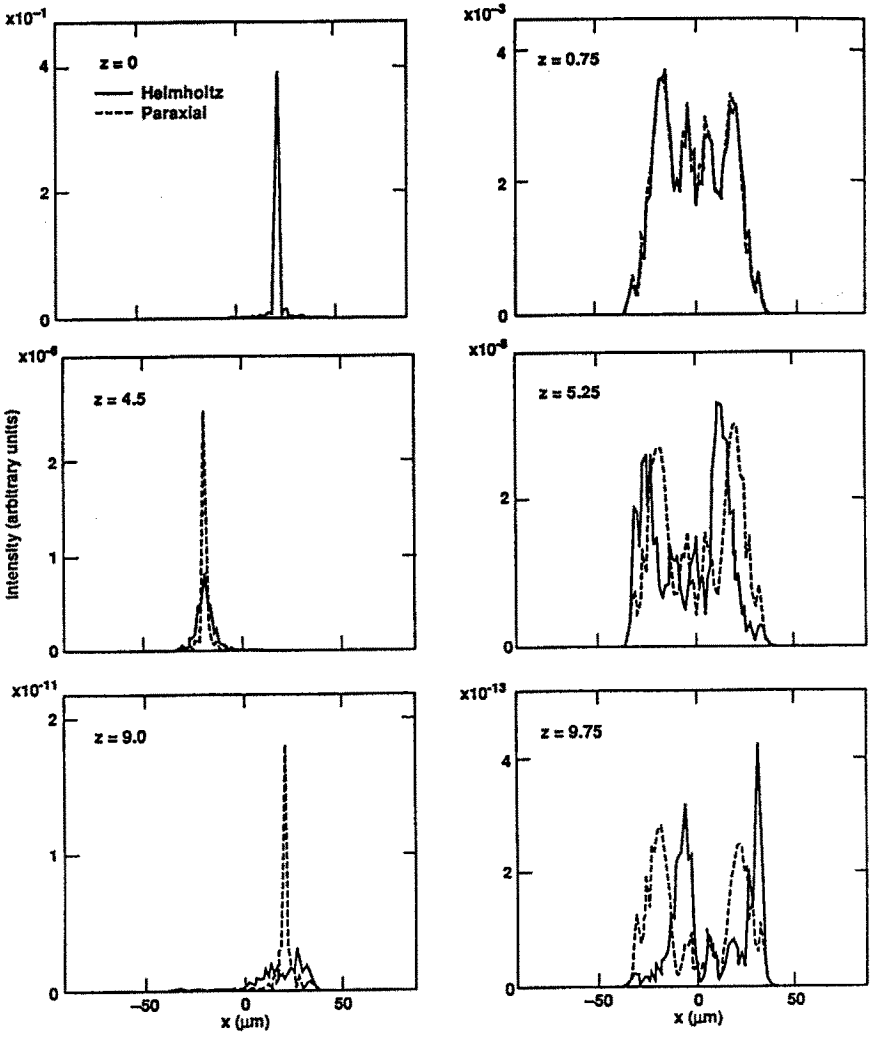

Figure 6. Comparison between Helmholtz and paraxial propagation in a quadratic refractive index waveguide with a quadratic absorption profile. Analytic and numerical solutions of Helmholtz equation are superimposed and indistinguishable.

Figure 5 shows the evolution of the beam as it propagates along the waveguide when ν is chosen so that profile (67) represents a quadratic gain profile. The propagation distance z is measured in units of the paraxial periodic focusing distance $Z_f = 0.146cm$ for the parabolic profile (67). The position of the beam oscillates back and forth about the center of the waveguide. The beam is narrow when it reaches its launching position, or its mirror image, but spreads out at the center of the waveguide. The analytic and numerical solutions, are superposed but indistinguishable. It was found that the difference between the on-axis analytic and the computed Helmholtz intensities was on the order of 10^6.

Figure 6 shows the corresponding results for the case of absorption, obtained by taking the sign of ν positive. The accuracy for the absorption case is comparable to that obtained for the gain case, and again the superposed analytic and numerical Helmholtz solutions are indistinguishable over fourteen orders of magnitude variation. The discrepancy between the Helmholtz and paraxial solutions is even greater than in the case of gain.

These examples demonstrate the effectiveness of the biorthogonal form of the Lanczos procedure for solving problems involving space dependent gain or absorption.

11. Propagation of Ultra Wide-Angle Beams in Homogeneous Media and the Importance of Evanescent Waves

Hermansson, *et. al.*, [18] reported that the Lanczos propagation method when applied to a rib-waveguide y-junction structure can result in slow and nonuniform convergence of the solution with respect to both longitudinal propagation step (z-step) and Lanczos order, when applied with the unapproximated square root propagation operator.

It has been shown [21] that the convergence problems referred to in [18] are not due to use of a square root operator, *per se*, but are due rather to the generation in the numerical solutions of evanescent field components that decay exponentially with z. We will find that an accurate description of wide-angle beam propagation with the Lanczos method is assured, even when formulated with an exponentiated square root operator, if the evanescent field components are avoided through

proper transverse zoning. Under these conditions the convergence of numerical error is uniform and longitudinal steps can be of the order of a wavelength.

As a stringent benchmark test of the Lanczos method we consider ultra wide-angle beam propagation in a two-dimensional uniform homogeneous medium with refractive index n_0. Computations will be relevant to radiation modes and can be tested against solutions obtained by the following method. In a homogeneous medium the Helmholtz equation becomes

$$\frac{\partial^2 \Psi}{\partial z^2} + \frac{\partial^2 \Psi}{\partial x^2} + k^2 n_0^2 \Psi = 0 \tag{73}$$

which can be solved to arbitrary accuracy in terms of the band-limited Fourier series

$$\Psi = \sum_{n=-N/2+1}^{N/2} \Psi_n e^{-i\beta_n z} e^{2\pi i n x/L} \tag{74}$$

Substituting (74) into (73) yields

$$\sum_{n=-N/2+1}^{N/2} \Psi_n e^{i\beta_n z} e^{2\pi i n x/L} \left[-\beta_n^2 - \left(\frac{2\pi n}{L}\right)^2 + k^2 n_0^2 \right] = 0 \tag{75}$$

For Eq. (75) to hold we must have

$$-\beta_n^2 - \left(\frac{2\pi n}{L}\right)^2 + k^2 n_0^2 = 0 \tag{76}$$

or

$$\beta_n = \sqrt{k^2 n_0^2 - \left(\frac{2\pi n}{L}\right)^2} \tag{77}$$

where the positive square root represents propagation in the positive direction.

Equation (77) implies that β_n is imaginary whenever

$$\frac{2\pi |n|}{L} > k n_0 \tag{78}$$

The corresponding Fourier coefficients will, as a consequence, decay exponentially with increasing z. These components represent evanescent waves, [22] which carry information about field variations over distances less than an optical wavelength. These components correspond to propagation angles that exceed 90 degrees and hence cannot propagate. One can insure that no Fourier component can decay exponentially by requiring that

$$\frac{\pi N}{L} \leq k n_0 \tag{79}$$

or, equivalently,

$$\Delta x \geq \frac{\lambda}{2 n_0} \tag{80}$$

Condition (80), which places a lower limit on the size of the transverse sampling increment Δx, implies that no feature smaller than a half-wavelength divided by the medium refractive index can be observed at distances where most of the the power in the evanescent Fourier components has decayed.

In the Lanczos solution to the Helmholtz equation the field is advanced in terms of the exponentiated square root propagation operator using

$$\Psi(\Delta z) = \mathbf{U}_M^{\dagger} \exp\left\{ ik\Delta z \left[1 - (1 + 2\boldsymbol{\beta}_M / k)^{1/2} \right] \right\} \mathbf{U}_M \Psi(0) \tag{81}$$

where M is the number of Lanczos vectors, $\boldsymbol{\beta}$ is an M-dimensional diagonal matrix, computed by diagonalizing the M-dimensional Lanczos matrix representation of the operator

$$H = \frac{1}{2k} \frac{\partial^2}{\partial x^2} \tag{82}$$

$\mathbf{U}_M$ is the M-dimensional unitary matrix that diagonalizes $\boldsymbol{\beta}_M$, and $k = n_0 \omega / c$. Some Lanczos eigenvalues β_m of the matrix $\boldsymbol{\beta}_M$ result in imaginary values for the square root in Eq. (81). Such eigenvalues correspond to evanescent field components in the Lanczos representation. It has been found that when the sampling rule (80) is satisfied, one obtains extremely close agreement between Fourier-Lanczos solutions and the band-limited Fourier series solution of Eqs. (73)–(77) for wide-angle propagation in a homogeneous medium. If the sampling condition

(80) is violated, agreement between the two methods deteriorates, unless very small longitudinal steps are taken, which suggests that the Lanczos representation does not accurately describe evanescent field components.

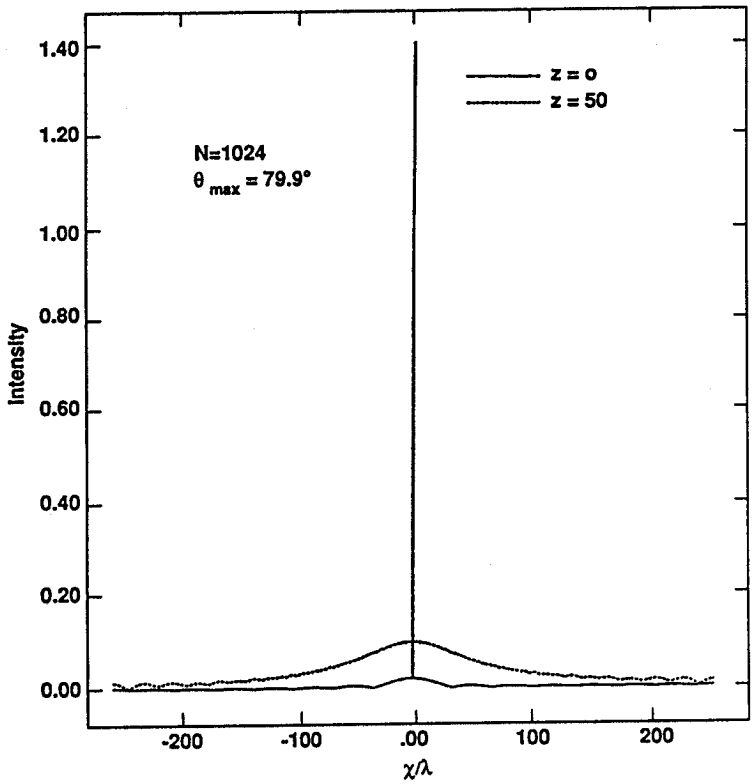

Figure 7. Lanczos propagation of an ultra wide-angle beam with maximum beam angle equal to 79.9° over distance of 50 wavelengths for $M = 16, \Delta z = \lambda$ and $\Delta x = \lambda/2$.

Figures 7–11 show the results of Lanczos-Fourier propagation of the initial delta-function-like beam

$$E(x, z = 0) = \sum_{n=N'/2+1}^{N'/2} e^{2\pi i n x/L} \tag{83}$$

calculated using 1024 sampling points, $n_0 = 1$, and $\Delta x = \lambda/2$. The value of N' in Eq. (81) was taken to be 1008, corresponding to a maximum beam angle of 79.9°, determined by the relation

$$\theta_{\max} = \sin^{-1}(N'/N) \tag{84}$$

where N is the total number of transverse grid points. Propagation covers the distance $z = 50\lambda$, with $\Delta z = \lambda$, $M = 16$, and $\lambda = 1\mu m$. Figure 7 shows the resulting beam intensities, before and after propagation, and Fig. 8 displays the Lanczos overlap error vs the longitudinal propagation step, Δz. The overlap error, $|1 - |\langle\psi(z)|\psi_L\rangle||$, is computed by projecting the Lanczos-Fourier solution onto the band-limited Fourier series solution, computed from Eqs (74)-(77) for the same grid. Clearly the Lanczos solution error converges uniformly with respect to both longitudinal z-step and Lanczos order M. In all cases the accuracy for a given order, as defined by the overlap error, saturates for a longitudinal step $\Delta z \cong \lambda$.

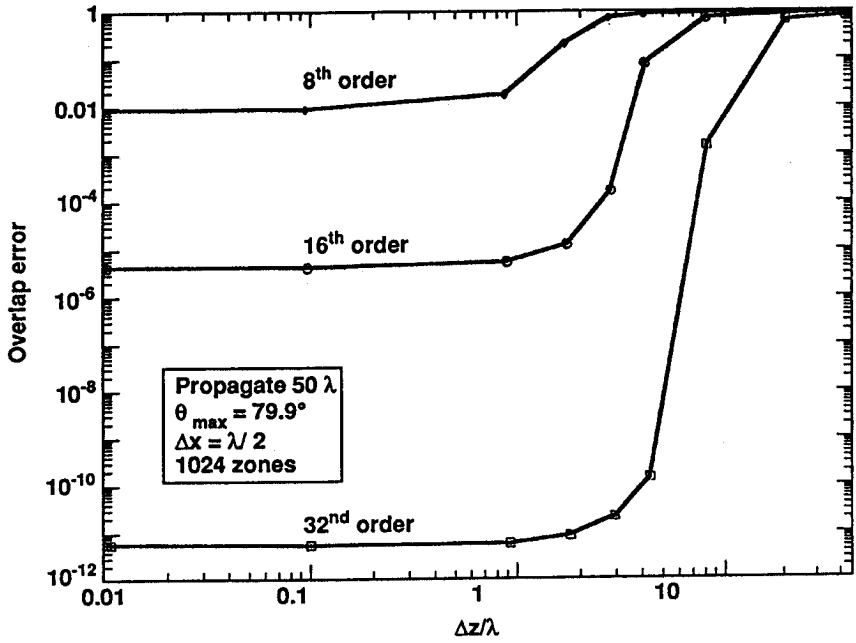

Figure 8. Overlap error as a function of z-step and Lanczos order (number of Lanczos vectors) for propagation in Figure 1.

Figure 9 shows the effect of violating condition (80) on the overlap error. The propagated field has been computed using $\Delta x = \lambda/4$, obtained by increasing the number of sampling points to 2048. Despite the increased sampling frequency the accuracy is actually reduced from that obtainable with $\Delta x = \lambda/2$ (also shown in Fig. 9). Furthermore, the overlap error does not display the saturation behavior close to $\Delta z \approx \lambda$ that is exhibited when $\Delta x = \lambda/2$.

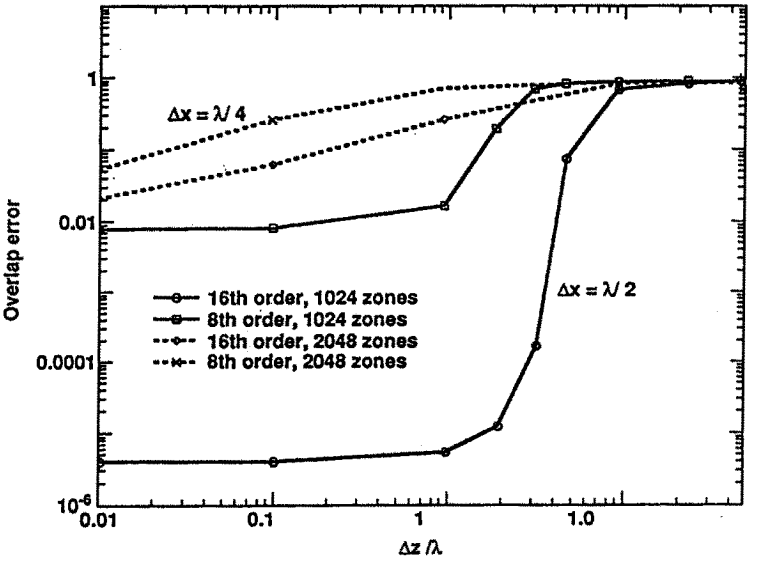

Figure 9. Comparison of overlap error for transverse zone sizes $\Delta x = \lambda/2$ and $\Delta x = \lambda/4$.

One might expect the Lanczos method applied in conjunction with a Taylor series approximation of the square root in Eq. (81) to yield accurate results, while, at the same time, removing the difficulties associated with imaginary values of the square root. The overlap error vs Δz for the propagation in Fig. 7 is plotted in Fig. 10 for a twelfth order Taylor series expansion. Also plotted in the same figure are results obtained with the unapproximated square root. The Taylor series approximation error converges rapidly with respect to both propagation step and Lanczos order, but to a sizeable error around 25%. Errors for the full square root operator are orders of magnitude smaller. These results imply that accuracy for very wide angle beam propagation, may require unacceptably high order Taylor approximations.

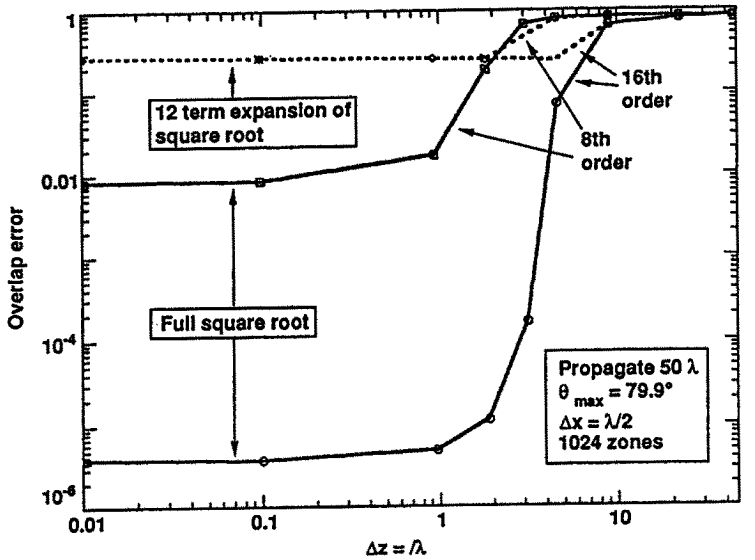

Figure 10. Comparison of Lanczos propagation overlap error for Taylor expansion of square root and unapproximated square root in propagation operator.

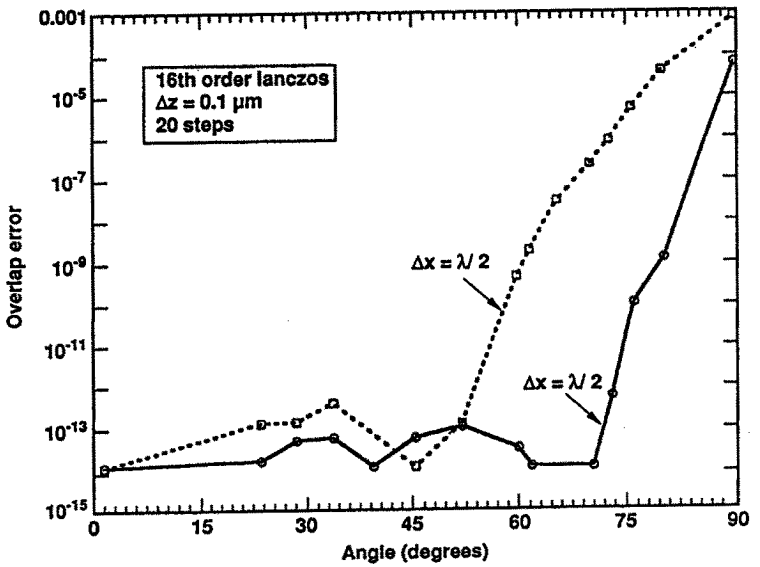

Figure 11. Overlap error for Lanczos propagation as a function of maximum beam angle, using two transverse sampling step steps.

Figure 11 shows the effect of transverse step size on the overlap error as a function of maximum beam angle, as determined by Eq. (84), for propagation of a beam of the form of Eq. (83) over the much smaller distance $z = 2\lambda$, with $N = 128$. For this example all overlap errors are smaller than the values encountered in the previous example. The smaller error magnitudes may be due to the significantly smaller propagation distance. In any case, a significant increase in the overlap error results when the transverse step size is decreased from $\Delta x = \lambda/2$ to $\Delta x = \lambda/4$ for beam angles greater than about $50°$. These results suggest that restrictions on transverse step size may be necessary only when very large angle components are present in the beam.

It has been demonstrated that the Lanczos method, applied in conjunction with the Helmholtz exponentiated square root operator, can accurately describe ultra wide-angle beam propagation in homogeneous media with acceptable longitudinal step sizes, provided that transverse step sizes are appropriately bounded from below. For propagation in inhomogeneous media the optimum transverse step size may not always be practical, but the implication of the results described here is that the most judicious use of Lanczos propagation, when radiation modes are involved, should emphasize economy rather than oversampling in transverse zoning.

12. Summary and Conclusion

We have described the Lanczos reduction scheme, which can be applied to solving the paraxial wave equation or for determining one way propagation solutions to the Helmholtz equation. Our discussion has been restricted in this chapter to solutions of the Helmholtz equation for longitudinally invariant refractive index distributions, which permit comparison between numerical and analytic solutions for determining accuracy. The tests that we have described indicate the possibility of high accuracy for the Lanczos reduction method in both its Hermitian and nonHermitian forms.

The Lanczos reduction scheme should also be applicable to refractive indices with weak longitudinal variation. A full discussion of these applications would take us well beyond the scope of this chapter. Needless to say, much research needs to be done on this new propagation method, but results obtained thus far indicate that the method has a promising future.

Acknowledgment

The author is indebted to M. D. Feit for a critical reading of the manuscript. This work was performed under auspices of the U. S. Department of Energy by the Lawrence Livermore National Laboratory under contract No. W-7405-ENG-48.

References

1. Fleck, Jr., J. A., J. R. Morris, and M. D. Feit, "Time-dependent propagation of high energy laser beams through the atmosphere," *Appl. Phys.*, Vol. 10, 129–160, 1976.
2. Huang, W. P., S. T. Chu, A. Goss, and S. K. Chaudhuri, "A scalar finite-difference time-domain approach to guided wave optics," *IEEE Photonics Tech. Lett.*, Vol. 3, 524–526, 1991.
3. Claerbout, J. F., *Fundamentals of Geophysical Data Processing with Applications to Petrolelum Prospecting*, McGraw-Hill, New York, 1976.
4. Lee, D., Y. Saad, and M. H. Schultz, "An efficient method for solving the three-dimensional wide angle wave equation," in *Computational Acoustics*, Vol 1 - Wave Propagation, Eds. D. Lee, R. L. Sternberg, and M. H. Schultz, North Holland, Amsterdam, 1988.
5. Feit, M. D. and J. A. Fleck, Jr., "Light propagation in graded-index optical fibers," *Appl. Opt.*, Vol. 17, 3990–3998, 1978.
6. Van Roey, J., J. van der Donk, and P. E. Lagasse, "Beam propagation method: analysis and assessment," *J. Opt. Soc. Amer.*, Vol. 71, 803–810, 1981.
7. Feit, M. D., and J. A. Fleck, Jr. "Beam paraxiality, filament formation, and beam breakup in the self-focusing of optical beams," *J. Opt. Soc. Amer. B*, Vol. 5, 633–640, 1988.
8. Thomson, D. J., and N. R. Chapman, "A wide-angle split-step algorithm for the parabolic equation," *J. Acoust. Soc. Amer.*, Vol. 74, 1848–54, 1983.
9. Thylén, L., and C. M. Lee, "Beam-propagation method based on matrix diagonalization," *J. Opt. Soc. Am. A*, Vol. 9, 143–146, 1992.
10. Gerdes, J., and R. Pregla, "Beam propagation algorithm based on the method of lines," *J. Opt. Soc. Am. B*, Vol. 8, 389–395, 1991.

11. Lanczos, C., "An iteration method for the solution of the eigenvalue problem of linear differential and integral operators," *J. Res. Nat Bur. Standards*, Vol. 45, 255–282, 1950.
12. Park, T. J., and J. C. Light, "Unitary quantum time evolution by iterative Lanczos reduction," *J. Chem. Phys.*, Vol. 85, 5870–5876, 1986.
13. Sehmi, B. S., *Large Order Structural Eigenanalysis for Finite Element Systems*, Halsted, New York, 1989.
14. Leforestier, C., R. H. Bisseling, C. Cerjan, M. D. Feit, R. Friesner, A. Goldberg, A. Hammerich, G. Jolicard, W. Karrlein, H. D. Meyer, N. Lipkin, O. Roncero, and R. Kosloff, "A comparison of different propagation schemes for the time dependent Schrödinger equation," *J. Comp. Phys.* Vol. 94, 59–80, 1991.
15. Ratowsky, R., and J. A. Fleck, Jr., "Accurate numerical solution of the Helmholtz equation by iterative Lanczos reduction," *Opt. Lett.*, Vol. 16, 787–789, 1991.
16. Ratowsky, R., J. A. Fleck, Jr., and M. D. Feit, "Helmholtz beam propagation in rib waveguides and couplers by iterative lanczos reduction," *J. Opt. Soc. Amer. A*, Vol. 9, 265–273, 1992.
17. Ratowsky, R., J. A. Fleck, Jr., and M. D. Feit, "Accurate solution of the Helmholtz equation by Lanczos orthogonalization for media with loss or gain," *Opt. Lett.*, Vol. 17, 10–12, 1992.
18. Hermansson, B., D. Yevick, W. Bardyszewski, and M. Glasner, "A comparison of Lanczos electric field propagation methods," *J. Lightwave Technol.*, Vol. 10, 772–776, 1992.
19. Feit, M. D., J. A. Fleck, Jr., and A. Steiger, "Solution of the Schrödinger equation by a spectral method," *J. Comp. Phys.* Vol. 47, 412–433, 1982.
20. Feit, M. D., and J. A. Fleck, Jr.,"Computation of mode eigenfunctions in graded-index optical fibers by the propagating beam method," *Applied Opt.*, Vol. 19, 2240-=2246, 1980.
21. Ratowsky, R., J. A. Fleck, Jr., and M. D. Feit, "Accurate description of ultra wide-angle beam propagation in homogeneous media by Lanczos orthogonalization," *Opt. Lett.*, in press.
22. Born, M., and E. Wolf, *Principles of Optics*, Pergamon, New York, p. 560, 1970.